

Structural and Biochemical Characterization of Levan Produced by *Gluconobacter cerinus* UELBM11 Isolated from Brazilian Grapes

Natália N. Y. Hata,^{1a} Daniele Sartori,^{2b} Matheus M. Ribeiro,^{2b} Rodrigo V. Serrato,^{3c} Adriana Aparecida B. Tomal,^{4d} Leonel Vinícius Constantino,^{5e} Mariana A. Q. Cancian,^{6a} Francisco A. Marques,^{7d} *f Fernando T. Hata,^{8g} Fernanda Carla H. Bana,^{9a} Fernando Macedo Jr.^{9e} and Wilma Aparecida Spinosa^a

^aLaboratório de Prestação de Serviços, Departamento de Ciência e Tecnologia de Alimentos, Universidade Estadual de Londrina, 86057-970 Londrina-PR, Brazil

^bLaboratório de Genética Toxicológica, Departamento de Bioquímica e Biotecnologia, Universidade Estadual de Londrina, 86057-970 Londrina-PR, Brazil

^cLaboratório de Química de Carboidratos e Glicoconjugados, Departamento de Bioquímica e Biologia Molecular, Universidade Federal do Paraná, 81531-990 Curitiba-PR, Brazil

^dLaboratório de Espectroscopia, Departamento de Ciências Naturais, Universidade do Estado de Minas Gerais, 35501-170 Divinópolis-MG, Brazil

^eLaboratório de Ecofisiologia e Biotecnologia Agrícola, Departamento de Química, Universidade Estadual de Londrina, 86057-970 Londrina-PR, Brazil

^fLaboratório de Ecologia Química e Síntese de Produtos Naturais, Departamento de Química, Universidade Federal do Paraná, 81531-990 Curitiba-PR, Brazil

^gLaboratório de Entomologia, Departamento de Agronomia, Universidade Estadual de Londrina, 86057-970 Londrina-PR, Brazil

Acetic acid bacteria (AAB) are versatile organisms that catalyze the conversion of a wide range of carbon sources into biomolecules of great industrial interest. In this study, we exploited the ability of *Gluconobacter* spp. to synthesize levans. Among the isolated strains, *Gluconobacter cerinus* UELBM11 produced approximately 14.0 g L⁻¹ of levan under non-optimized conditions. Gas chromatography-mass spectrometry (GC-MS), Fourier transform infrared spectroscopy (FTIR), and nuclear magnetic resonance (NMR) analyses confirmed that levan obtained from *G. cerinus* UELBM11 consisted of a β -(2 \rightarrow 6)-D-fructose backbone with some β -(2 \rightarrow 1) ramifications. The average molecular weight (Mw) of the purified levan was 8.78 \times 10⁵ Da. Thermogravimetric/differential thermogravimetric (TGA/DTG) analysis indicated high thermal stability, with the maximum decomposition rate observed at 227.44 °C. Scanning electron microscopy (SEM) revealed a microporous morphology, and the antioxidant activity assays demonstrated that levan had a high scavenging capacity of 2,2'-azino-bis (3-ethylbenzothiazoline-6-sulfonic acid) (ABTS) and hydroxyl radicals. Therefore, it has been demonstrated the levan produced by *G. cerinus* UELBM11 is a promising natural antioxidant and, owing to its microporosity and excellent thermal properties and stability, is a potential candidate as an additive in cosmetics, pharmaceuticals, and food products.

Keywords: acetic acid bacteria, fructan, biotechnology

Introduction

Acetic acid bacteria (AAB) are well-known spoilage microorganisms that can easily be isolated from foods or

beverages such as wine, beer, sweet drinks, and fruits.^{1,2} Naturally spoiled grapes are an excellent medium for AAB proliferation because the sugars and alcohols therein can be quickly oxidized to organic acids. Furthermore, under these conditions, the tolerance of AAB to ethanol and its ability to convert it into acetic acid hamper the multiplication of several other microorganisms.³ Additionally, AAB are

*e-mail: fassismarques@yahoo.com.br

Editor handled this article: Hector Henrique F. Koolen (Associate)



versatile organisms of enormous industrial interest, as they play a major role in producing ascorbic acid (vitamin C) and bacterial cellulose. These bacteria are involved in the manufacturing of several food industry products, including vinegar, cocoa, kombucha, and other similar fermented beverages.¹

Recently, AAB species of the genera *Asaia*, *Gluconobacter*, *Gluconacetobacter*, *Komagataeibacter*, *Kozakia*, *Neoasaia*, and *Tanticharoenia* have been analyzed for their ability to produce levan-type fructans with multiple applications.⁴ Levans are homopolysaccharides constituted by a backbone of D-fructose units linked by β -(2 \rightarrow 6)-glycosidic bonds, sometimes with β -(2 \rightarrow 1)-linked sidechains, and bearing a terminal non-reducing D-glucosyl residue.⁵ The biosynthesis of bacterial levan is catalyzed by levansucrase (EC 2.4.1.10), an enzyme belonging to the family of glycoside hydrolases (GH68) that catalyzes the hydrolysis of sucrose and the transfer of fructosyl units to various acceptors.^{6,7}

The unique properties presented by levans, such as high solubility in water and oil, strong adhesiveness, biocompatibility, and film-forming ability, make these polysaccharides a potential functional biopolymer of commercial interest, especially for the food, cosmetics, and pharmaceutical industries.⁸ Levans are also considered prebiotic effectors since they modulate the composition and function of the human colon microbiota, increasing the growth of probiotic strains.⁹ In bread making, Jakob *et al.*¹⁰ used levans obtained from AAB and reported a significant increase in volume, reduced crumb hardness, and retarded staling of wheat bread. Other applications of levans in food include their use as emulsifying additives, fat substitutes, and encapsulating and stabilizing agents.^{8,11} Levans have a wide range of biological activities, such as antioxidant,¹² anti-inflammatory,¹² hypocholesterolemic,¹¹ immunomodulatory,⁴ anticancer,^{13,14} and curative effects on peptic ulcers¹⁵ in the biomedical area.

Considering the wide potential for levan applications and the fact that its production from AAB is still relatively recent, the pursuit of novel and more potent producing strains is extremely relevant for obtaining higher yields and diminished production costs. Moreover, levans produced from different microbial sources may differ in their fine structures, affecting their physicochemical and bioactive properties. Therefore, we isolated *Gluconobacter* strains from Brazilian grapes that can produce exopolysaccharides (EPS), tested their ability to synthesize homopolysaccharides from sucrose, and chemically characterized the levans produced by *G. cerinus* strain UELBM11. Furthermore, the *in vitro* antioxidant activity of the isolated levan was determined

using 2,2'-azino-bis (3-ethylbenzothiazoline-6-sulfonic acid) (ABTS) and hydroxyl radical-scavenging assays.

Experimental

Microorganism isolation

Over-ripe grape (*Vitis labrusca* L.) samples were collected from two different areas in Brazil: Barreiras, Bahia (11°57'14.0"S, 45°31'51.7"W) and Sarandi, Paraná (23°25'00.4"S, 51°48'58.3"W). The samples were cut into small pieces and separately inoculated in two enriched culture media. i.e., MYP (manitol (Labsynth, Diadema, Brazil), yeast extract (Himedia, Mumbai, India), and peptone (Himedia, Mumbai, India))¹⁶ and GEPYA (glucose (Labsynth, Diadema, Brazil), ethanol (Labsynth, Diadema, Brazil), peptone (Himedia, Mumbai, India), yeast extract (Himedia, Mumbai, India), acetic acid (Êxodo científica, Sumaré, Brazil), and cycloheximide (Êxodo científica, Sumaré, Brazil)).¹⁷ Samples were incubated under aerobic conditions at 30 °C (Tecnal, São Paulo, Brazil) for 120 h. After incubation, serial dilutions were prepared from both culture media and spread onto MYP agar plates. The plates were incubated at 30 °C for 96 h, and bacterial colonies were isolated by repeated streaking. All isolates were stored in 20% (m/v) malt extract medium (Himedia, Mumbai, India) at -20 °C.

Biochemical and morphological identification of bacterial strains

Morphological and biochemical analyses were carried out according to Bergey's Manual of Systematic Bacteriology^{18,19} and other reports.^{10,20-22} First, Gram staining and ethanol oxidation tests were performed to identify the AAB isolates. Only Gram-negative strains that produced acetic acid were subjected to the catalase production test, production of cellulose, production of dihydroxyacetone from glycerol (ketogenesis), production of brown pigment, acid production from glucose, over-oxidation of acetic acid to carbon dioxide and water, oxidation of lactate to carbon dioxide and water, and production of mucus EPS on sucrose agar plates. EPS-producing strains were identified macroscopically and classified as: (+) weak, (+++) strong, or (-) no production of mucous EPS from sucrose, according to Jakob *et al.*¹⁰

Molecular identification

Molecular techniques for species identification were performed only for isolates that demonstrated (+++) strong EPS-producing capacity.

DNA extraction

A cell suspension in sterile ultrapure water (1.0 mL) was prepared from a fresh culture on MYP agar for the analysis of each strain. Deoxyribonucleic acid (DNA) extraction from the bacteria was performed as described by Cheng and Jiang.²³ The quantification of extracted DNA was estimated by electrophoresis on 1% (m/v) (Ludwig Biotec, Alvorada, Brazil).

Polymerase chain reaction (PCR) amplification

PCR primers (Exxtend, Paulínia, Brazil) employed to amplify the 16S rDNA were 16Sd 5'-GCTGGCGGCATGCTTAACACAT-3' and 16Sr 5'-GGAGGTGATCCAGCCGCAGGT-3'.²⁴ The reaction mixture (25 μ L) contained 10 ng bacterial DNA, 0.4 μ mol L⁻¹ of each primer, 0.25 mmol L⁻¹ of the dNTPs mix, 2.0 mmol L⁻¹ MgCl₂, 1 U Taq DNA polymerase, amplification buffer (Invitrogen, Carlsbad, CA, USA) and ultrapure water. PCR was performed in a thermal cycler (Eppendorf, Hamburg, Germany), and amplification was conducted as described by Ruiz *et al.*²⁴ Amplified PCR products were checked using 1% (m/v) agarose gel (Ludwig Biotec, Alvorada, Brazil) electrophoresis using 1 kb DNA Ladder markers. Purified PCR products were sequenced by Biotecnologia Pesquisa e Inovação (Brazil). The sequences were aligned with previously determined sequences deposited in the National Center for Biotechnology Information database²⁵ using the software MEGA 7.²⁶ Phylogenetic tree reconstruction was performed using the neighbor-joining method. All the identified bacteria were registered in GenBank.

Cultivation of selected strains and production of levans

All the identified strains were evaluated for their ability to produce fructose EPS from growth media containing sucrose. Firstly, one loopful of pre-inoculum cultivated for 72 h on MYP agar (1%, m/v) was transferred to 250 mL flasks containing 100 mL of HS medium (2.0% m/v glucose (Labsynth, Diadema, Brazil); 0.5% m/v peptone (Himedia, Mumbai, India); 0.5% m/v yeast extract (Himedia, Mumbai, India); 0.27% m/v anhydrous disodium phosphate (Labsynth, Diadema, Brazil); 0.115% m/v monohydrate citric acid (Labsynth, Diadema, Brazil); pH 6.0).²⁷ After cultivation, the samples were incubated at 30 °C on a rotary shaker (120 rpm) (TECNAL-4200, Piracicaba, Brazil) until 0.6 of absorbance (600 nm) (Thermo Electron Corporation Spectronic Genesys 6, Madison, WI, USA). The cells were then washed and used as inoculum. Levan production during fermentation was performed in Erlenmeyer flasks with a working volume of 100 mL. Modified HS medium

(50 g L⁻¹ sucrose (Labsynth, Diadema, Brazil)) was inoculated with standardized inoculum (1%, v/v) and incubated at 30 °C for 48 h under shaking conditions (150 rpm) (TECNAL-4200, Piracicaba, Brazil).

Isolation, purification, and quantification of levans

The fermentation process was interrupted by centrifugation at 5000 rpm (Centrifuge 5804 R, Eppendorf, Hamburg, Germany) for 20 min to remove the cells. The supernatant obtained was then precipitated with cold ethanol 99% (3:1, v/v) and left overnight at -20 °C.²⁸ The precipitate formed was recovered by centrifugation and let it to dry at 50 °C (partially purified levan). Prior to identification and structural characterization, partially purified levan was redissolved in ultrapure water, followed by deproteinization with 1% Alcalase 2.4L FG (v/v) (Novozymes Latin American Limited, Araucária, PR, Brazil) at pH 8.0 and incubation at 55 °C for 90 min. After the procedure, the solution was incubated at 85 °C for 10 min to inactivate the enzyme, centrifuged, and the supernatant reprecipitated with ethanol, dialyzed (MWCO 14 kDa) (Sigma-Aldrich, St. Louis, MO, USA) for 48 h against distilled water at 4 °C, and lyophilized (CHRIST Alpha 1-2 LD Plus Lyophilizer, Osterode am Harz, Germany).¹⁰

The dry sample was dissolved in deionized water, loaded onto a Sepharose CL-2B (Sigma-Aldrich, St. Louis, MO, USA) column (20 mm \times 500 mm) and eluted with 50 mmol L⁻¹ phosphate buffer (pH 7.0) at a flow rate of 0.5 mL min⁻¹. The main fractions were detected using the phenol-sulfuric acid method²⁹ and pooled, dialyzed, and lyophilized as previously described (purified levan). The protein content was estimated using the Bradford method with bovine serum albumin (Sigma-Aldrich, St. Louis, MO, USA) as the standard.³⁰

For quantification, the purified levans were analyzed using high-performance anion-exchange chromatography/pulsed amperometric detection (HPAEC-PAD ICS 5000) (Dionex Canada Ltd., Oakville, Canada) equipped with a CarboPac PA-10 column (250 mm \times 4 mm) (Dionex, Sunnyvale, CA, USA). Briefly, levan was resuspended and hydrolyzed in 0.05 mol L⁻¹ oxalic acid for 1 h at 100 °C³¹ neutralized with 0.1 mol L⁻¹ NaOH (Sigma-Aldrich, St. Louis, MO, USA) and filtered through a 0.22 μ m membrane (Millipore, Bedford, MA, USA). Aliquots of 10 μ L were analyzed at a flow rate of 1 mL min⁻¹ at 25 °C with isocratic elution of 20 mmol L⁻¹ NaOH through the use of ultrapure water (resistivity of 18.2 M Ω , 90% solvent A) and 200 mmol L⁻¹ NaOH (10% solvent B) (Sigma-Aldrich, St. Louis, MO, USA) for 20 min. A regeneration step with 200 mmol L⁻¹ NaOH (10 min),

followed by re-equilibration with 20 mmol L⁻¹ NaOH for 15 min was performed for each chromatographic run. Fructose and glucose (Sigma-Aldrich, St. Louis, MO, USA) standards treated under the same conditions were used for quantification.

Structural characterization of levan from *Gluconobacter cerinus* UELBM11

Molecular weight determination

Molecular mass was determined using high-pressure steric exclusion chromatography (HPSEC) with four gel permeation ultrahydrogel columns (2000, 500, 250, and 120) (Waters Corporation, Milford, MA, USA), eluted in series. This system was equipped with a differential refractive index (IR) detector and a multi-angle laser light scattering detector (MALLS) (Wyatt Technology, Santa Barbara, CA, USA). Levan samples were prepared and analyzed according to the procedure described by Serrato *et al.*²⁸ Differential refractive index of the solvent-solute solutions (dn/dc) was determined using levan solutions with different concentrations (0.1, 0.2, 0.4, 0.6, 0.8 and 1.0 mg mL⁻¹), prepared in 100 m mol L⁻¹ NaNO₂ (Merck KGaA, Darmstadt Hesse, Germany) containing 0.02% NaN₃ (Sigma-Aldrich, St. Louis, MO, USA) and filtered through a 0.22 μm nitrocellulose membrane before sequential injection (0.5 mL) of each solution in increasing order of concentration. Experiments were carried out at 25 °C with flow rate of 600 μL min⁻¹. Light scattering signal was detected simultaneously at 11 scattering angles ranging from 35° and 132°. The collected data were analyzed with the ASTRA software 4.70.07 (Wyatt Technology, Santa Barbara, CA).³²

Fourier-transform infrared (FTIR) spectroscopy

The functional groups and chemical bonds of levans were determined using FTIR spectroscopy (Shimadzu, Kyoto, Japan). The sample was prepared as a KBr pellet, and the spectroscopic measurements were carried out within the wavelength range of 400-4000 cm⁻¹ with a resolution of 4 cm⁻¹.

Monosaccharide composition analysis

The monosaccharide composition of the purified levan was identical to that of its alditol acetate (AA) derivative. Levan was firstly hydrolyzed with 2 mol L⁻¹ trifluoroacetic acid (Sigma-Aldrich, St. Louis, MO, USA) (30 min, 50 °C),³³ followed by reduction with excess sodium borohydride (Sigma-Aldrich, St. Louis, MO, USA) for 12 h and then acetylated with a mixture of pyridine (Sigma Aldrich, St. Louis, MO, USA) and acetic anhydride

(Sigma Aldrich, St. Louis, MO, USA) (1:1 v/v) for 24 h at 120 °C. The alditol acetates obtained were extracted with chloroform, washed successively with 5% CuSO₄ solution (m/v) (CuSO₄·5H₂O, Labsynth, Diadema, Brazil) to remove residual pyridine, and then washed with water twice. The resulting organic phase was then dried and subjected to gas chromatography-mass analysis (GC-MS) (Varian CP-3800 GC) (Agilent Technologies, Santa Clara, CA, USA) according to Serrato *et al.*²⁸ A DB-1 capillary column (30 m × 0.25 mm internal diameter (i.d.)) (Agilent Technologies, Santa Clara, CA, USA) was used and the temperature program was set from 100 to 140 °C (5 °C min⁻¹), then increasing to 240 °C (4 °C min⁻¹) and held for 10 min, with He as carrier gas (grade 5.0, 1.0 mL min⁻¹).²⁸ The injector was kept at 260 °C and in-line mass spectrometry was performed using a flame ionization detector (FID), with a hydrogen/synthetic air flame (260 °C).²⁸

Per-O-methylation analysis

Linkage analysis of the levan monosaccharide units was performed according to the method described by Gojgic-Cvijovic *et al.*³⁴ Briefly, levan (60 mg) was dissolved in anhydrous dimethyl sulfoxide (Labsynth, Diadema, Brazil) with excess NaOH (Labsynth, Diadema, Brazil) and fully methylated with iodomethane (Sigma-Aldrich, St. Louis, MO, USA). The resulting material was dialyzed (MWCO 14 kDa) against distilled water and hydrolyzed with 1% acetic acid (Anidrol, Diadema, Brazil) at 100 °C for 4 h;³⁵ reduction and acetylation were performed as previously described. Partially methylated alditol acetate (PMAA) monosaccharide derivatives were determined by GC-MS analysis (Varian Saturn Ion Trap 2000 GC-MS system with a CP-3800 GC) (Agilent Technologies, Santa Clara, CA, USA), and conditions were as described by Sasaki *et al.*³⁶ A DB-225 capillary column (30 m × 0.25 mm i.d.) (Agilent Technologies, Santa Clara, CA, USA) was used for elution with He (grade 5.0, 20 cm min⁻¹/0.05 mL min⁻¹). Injector temperature was 250 °C, initial temperature set to 50 °C for 1 min, ramping up to 215 °C (40 °C min⁻¹) and held for 40 min. Electron impact was at 70 eV.³⁶

Nuclear magnetic resonance (NMR)

The type of linkage in the biosynthesized levans was identified using ¹H and ¹³C NMR analyses. 0.5 mL of purified aqueous levan (30 mg mL⁻¹) was diluted with 0.1 mL of deuterium oxide (99.9% atom D; Sigma-Aldrich) and transferred to a 5 mm broadband probe head operating at 400.13 MHz for ¹H and 100.13 MHz for ¹³C in an NMR spectrometer (Bruker Avance III, Karlsruhe, Germany). All

^1H NMR spectra were recorded at 25 °C using a standard presaturation pulse sequence (“zgpr”, Bruker) to suppress strong $\text{H}_2\text{O}/\text{HDO}$ signal using 128 scans, each of them with acquisition time of 4.1 s, relaxation delay of 1 s and a low power pulse set on the water resonance. Chemical shifts (δ) were expressed in ppm.

Thermogravimetric analysis (TGA) and differential thermogravimetric analysis (DTG)

Thermogravimetric analysis (TGA) was performed using a TGA-50 analyzer (Shimadzu, Tokyo, Japan) under an N_2 atmosphere at a flow rate of 20 mL min^{-1} . The sample was placed in a crucible and heated at a linear heating rate of 10 °C min^{-1} over a temperature of 30-800 °C. DTG was applied to derivatize the levan TGA data.

Scanning electron microscopy (SEM)

Scanning electron microscopy was used to investigate the morphology of the levan. Micrographs of the samples coated with a thin layer of gold nanoparticles were obtained using a Quanta 200 scanning electron microscope (FEI, Hitachi, Japan).

Antioxidant activity

ABTS free radical scavenging activity

ABTS radical scavenging activity was determined according to the method described by Huang *et al.*³⁷ with some modifications. Firstly, 7 mmol L^{-1} ABTS (Sigma Chemical Co., St. Louis, MO, USA) and 140 mmol L^{-1} potassium persulfate solutions (Labsynth, Diadema, Brazil) were prepared in ultrapure water. Then, 5 mL 7 mmol L^{-1} ABTS and 88 μL 140 mmol L^{-1} potassium persulfate solutions were reacted in the dark for 16 h to generate the ABTS radical (ABTS^{•+}). The ABTS^{•+} solution was diluted with 20 mmol L^{-1} monobasic potassium phosphate (pH 7.4) (Labsynth, Diadema, Brazil) to obtain an absorbance of 0.70 ± 0.02 at 734 nm. The analysis consisted of 100 μL of aqueous levan solution added to 1000 μL of diluted ABTS^{•+} solution. The reaction mixture containing different concentrations of levan (0, 0.05, 0.09, 0.18, 0.27, 0.36, 0.45, and 0.91 mg mL^{-1}) was incubated in the dark for 6 min at room temperature, and the absorbance was measured at 734 nm. The ABTS^{•+} scavenging activity was calculated using the following equation:

$$\text{Radical scavenging activity (\%)} = \frac{(\text{Abs. control} - \text{Abs. sample})}{(\text{Abs. control})} \times 100 \quad (1)$$

where Abs. control is the absorbance of ABTS^{•+} without the sample and Abs was used as the control. The absorbance of the sample solution was used as the sample. Vitamin C

(Labsynth, Diadema, Brazil) was used as the positive control.

Hydroxyl radical scavenging activity assay

The ability of levans to scavenge the hydroxyl radicals generated by the Fenton reaction was assayed as described by Gomaa and Yousef³⁸ with some modifications. Levan solutions (1.0 mL) were added to 1.0 mL of 9 mmol L^{-1} ferrous sulfate (m/v) (Labsynth, Diadema, Brazil), 1.0 mL of 0.3% H_2O_2 (v/v) (Labsynth, Diadema, Brazil), and 0.5 mL of 9 mmol L^{-1} salicylic acid/ethanol solution (m/v) (Labsynth, Diadema, Brazil). The mixture containing different concentrations of levan (0, 0.14, 0.29, 0.57, 0.86, 1.14, 1.43, and 2.86 mg mL^{-1}) was incubated at 37 °C for 30 min, and the absorbance of the samples was measured by spectrophotometer at 510 nm (Thermo Electron Corporation Spectronic Genesys 6, Madison, WI, USA). Vitamin C (Labsynth, Diadema, Brazil) was used for comparison purposes. Hydroxyl radical scavenging activity was calculated using equation 1.

Statistical analysis

The results were analyzed using one-way analysis of variance (ANOVA) and Tukey’s test ($p \leq 0.05$) using the Statistica 10.0 software (StatSoft Inc., Tulsa, USA),³⁹ and the graphical analysis was performed by using GraphPad Prism software v. 5.00 (GraphPad Software, San Diego, USA),⁴⁰ and OriginPro 8 software (OriginLab Corporation, Northampton, USA).⁴¹

Results and Discussion

Identification and selection of levan-producing *Gluconobacter* strains

A total of 42 bacterial strains were isolated from rotten grapes in the Bahia and Paraná states. All analyzed bacteria exhibited Gram-negative staining and the capacity to oxidize ethanol to acetic acid (data not shown). Based on morphological, physiological, and biochemical characteristics and EPS production, five AAB isolates were identified and demonstrated (+++) strong activity on sucrose agar plates (Table S1, Supplementary Information (SI) section). Figure S1 in the SI section shows that all isolates belonged to the genus *Gluconobacter*.

The bacterial cells were rod-shaped, non-spore-forming, and catalase-positive, as described in Bergey’s Manual of Systematic Bacteriology.¹⁹ *Gluconobacter* isolates could convert ethanol to acetic acid, but not acetate or lactate, into CO_2 and H_2O . The conversion of acetate to CO_2 and H_2O ,

which is known as acetate “overoxidation,” is commonly found in some genera of AAB, such as *Acetobacter*, *Gluconacetobacter*, and *Komagataeibacter*. However, this ability is absent in *Gluconobacter* owing to a lack of key enzymes in the tricarboxylic acid cycle and glyoxylate pathway.^{3,22} Likewise, *Acetobacter* readily converts lactate to CO₂ and H₂O, whereas *Gluconobacter* preferentially oxidizes carbohydrates to produce acetic acid.^{21,22} All the strains analyzed herein produced organic acids from glucose and dihydroxyacetone from glycerol, but none of them were able to produce cellulose. Furthermore, the formation of water-soluble brown pigments was not observed in any of the isolates. This characteristic varies among species²⁰ and is linked to the synthesis of 2,5-diketogluconic acid and γ -pyrones from D-glucose.¹⁹ Similar to our findings, Jakob *et al.*¹⁰ also demonstrated that *G. cerinus* DSM 9533 and *G. frateurii* TMW 2.767 have a strong activity of EPS production (+++).

All five AAB isolates were identified using DNA sequencing and phylogenetic analysis of the 16S rRNA gene. The UELBM13, UELMM2, UELBM1, UELBM11, and UELMM4 strains showed profiles similar to that of the *Gluconobacter* reference strains (Figure S1) and were later named and deposited in Genbank database, as *Gluconobacter frateurii* UELBM13 (GenBank accession No. ON149511), *Gluconobacter frateurii* UELMM2 (GenBank accession No. ON149512), *Gluconobacter cerinus* UELBM1 (GenBank accession No. ON149513), *Gluconobacter cerinus* UELBM11 (GenBank accession No. ON149510), and *Gluconobacter kondonii* UELMM4 (GenBank accession No. ON149514), respectively.

The production of an EPS-like mucous substance by the *Gluconobacter* genus has not yet been described in Bergey’s Manual. However, recent reports^{31,42} showed that these bacteria can synthesize large amounts of homopolysaccharides from sucrose. Thus, EPS production by AAB isolates in HS culture medium containing sucrose was analyzed. Sucrose-based substrates are required for microbial production of levans since levansucrase shows high specificity for this non-reducing disaccharide.⁶ In the experimental conditions used herein, the concentrations of levan produced by the isolated strains ranged from 4.68 to 13.89 g L⁻¹ (Table 1).

Although the fermentation conditions were not optimized, the production of levan from *G. cerinus* UELBM11 was very promising, as it was higher than or comparable to those previously found for *Brachybacterium phenoliresistens*⁴³ and *Acetobacter xylinum* NCIM 2526.¹² The purified levan obtained from *G. cerinus* UELBM11 was quantified and showed a yield of 11.68 g L⁻¹. Preliminary analysis using

Table 1. Production of levan on modified HS-medium from *Gluconobacter* strains

Strain	Levan yield / (g L ⁻¹)	Origin (Brazilian state)
<i>G. cerinus</i> UELBM11	13.89 ± 0.90 ^a	Bahia
<i>G. kondonii</i> UELMM4	12.60 ± 1.39 ^a	Paraná
<i>G. cerinus</i> UELBM1	10.80 ± 0.77 ^b	Bahia
<i>G. frateurii</i> UELMM2	9.52 ± 0.49 ^b	Paraná
<i>G. frateurii</i> UELBM13	4.68 ± 0.84 ^c	Bahia

Data represent mean ± standards deviations. Means with same letters in the same column are not significantly different by Tukey’s test at 5%.

FTIR and NMR confirmed that all strains could synthesize levans (data not shown); however, for the purposes of this study, only the levan produced by *G. cerinus* strain UELBM11 was chosen for fine structural characterization and biological activity analyses.

Structural characterization of the purified levan produced by *G. cerinus* UELBM11

Molecular weight and FTIR analyses

Purifying the levan obtained from strain UELBM11 of *G. cerinus* using a Sepharose CL-2B column showed a single peak at a measured absorbance of 490 nm (Figure S2, SI section). The collected fraction was checked for purity, and a negative result was obtained in the Bradford test, indicating the absence of proteins in the sample. Although levan-producing AAB are known to produce relatively high-molecular-weight homopolysaccharides (e.g., *N. chiangmaiensis* 100-575 Mda, *K. baliensis* 1000-2000 Mda, *G. frateurii* 4-98 Mda, *G. cerinus* 6-98 Mda),⁴⁴ HPSEC-MALLS analysis revealed that the levan produced by *G. cerinus* UELBM11 had a lower molecular weight of 8.78 × 10⁵ Da. Levan from another acetic acid bacterium, *Tanticharoenia sakaeratensis*, showed a similar result, in which the majority of molecular weight ranged from approximately 1 × 10⁵-6.8 × 10⁵ Da.⁴ The practical application of levans, whether as a bioactive, functional, or natural compound, is directly related to its molecular weight.^{45,46} According to Ortiz-Soto *et al.*,⁴⁶ the molecular weight of levans can be classified into two categories: low molecular weight (LMW; 8-50 kDa) and high molecular weight (HMW; > 50 kDa). In general, LMW levans can be used as potential prebiotic candidates to modulate the human intestinal microflora,⁹ whereas HMW levans have a broader variety of industrial applications. HMW levans have been used as a fat replacer in dairy products due to their mouthfeel, taste, and spreadability,¹¹ and strongly influence bread quality and staling rate.¹⁰ In the cosmetical and biomedical areas, HMW levans have

moisturizing properties,⁴⁷ hypocholesterolemic effects,⁴⁸ and antitumor activities and have shown great potential in nanocarrier systems for drug delivery.^{46,49} As for their antioxidant activities, both LMW and HMW levans present quite diverse responses.^{34,50-52}

The FTIR allows detailed analysis of the molecular structure of levans, providing valuable information, such as the presence of furanic or pyranose rings, as well as glycosidic bonds (type α or β), in addition to identifying the presence and type of branches in a main chain of levans. In this study, FTIR spectra of the purified levan samples (Figure 1) were analyzed and compared with the FTIR spectra of polysaccharides documented in the literature⁵³⁻⁵⁵ and absorption bands were assigned, indicating the typical polymeric structure of levan.

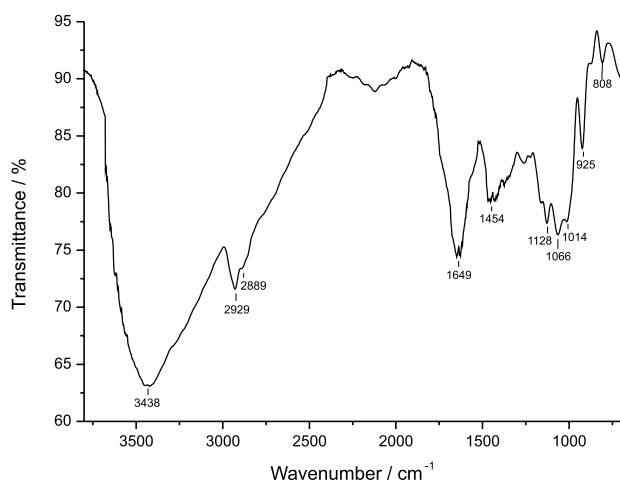


Figure 1. FTIR (KBr) spectrum of levan produced from *Gluconobacter cerinus* UELBM11.

The polysaccharide nature of the samples was confirmed by the wide absorption range in the region of 3400 cm^{-1} , resulting from the stretching vibration of the hydroxyl groups ($\nu\text{O-H}$). The bands observed in the regions close to 2930 and 2880 cm^{-1} were attributed to vibrations of symmetrical and asymmetric stretching of C-H bonds. Bands around 1650 cm^{-1} were assigned to the symmetrical angular deformation in the hydroxyl plane, related to fundamental water vibrations.⁵³ The FTIR spectra also

showed small bands at approximately 1450 cm^{-1} , which were attributed to angular deformation in the plane of methylene C-H bonds. The fingerprint region from 1200 to 800 cm^{-1} can be used to characterize different polysaccharides.⁵⁴ Bands near 1125 , 1065 , and 1015 cm^{-1} correspond to the stretches of the carbohydrate glycosidic bonds ($\nu\text{C-O-C}$) and ($\nu\text{C-O-H}$). The two characteristic signals at 925 and 808 cm^{-1} indicate the presence of furanoside rings in the sugar units, and these values correspond to the levan produced by *Bacillus licheniformis*.⁵⁵ The absence of bands of carboxylic groups and sulfate was also observed.

Monosaccharide composition and glycosidic linkage analysis

After derivatization of the levan produced by *G. cerinus* UELBM11 to yield alditol acetates (AA), GC-MS analysis revealed the presence of Man (51.6%) and Glc (48.4%) as the main monosaccharides in the polymer composition. This result was expected because the D-fructose units present in levans give rise to both epimers after reduction with sodium borohydride, and mannitol hexaacetate ($t_R = 18.83$ min), and glucitol hexaacetate ($t_R = 18.92$ min) were found on the chromatogram after hydrolysis, reduction, and acetylation of the purified levan sample.

The same phenomenon was observed when partially methylated alditol acetates (PMAA) were produced to determine the glycosidic linkage of D-fructose in the levan structure (Table 2 and Figure 2).

After derivatization, PMAA was analyzed using GC-MS, which showed two main peaks at 15.32 and 15.40 min, corresponding to the 1,3,4- Me_3 -Glc and 1,3,4- Me_3 -Man derivatives, respectively. Together, these 1,3,4- Me_3 -hexitol derivatives accounted for 86.13% of the PMAA found for the levan produced by *G. cerinus* UELBM11, and both represent the (2 \rightarrow 6)-linked Fruf residues that form the levan backbone.³³ Minor branching units of (1,2 \rightarrow 6)-linked Fruf were also observed since 3,4- Me_2 -hexitol (5.87%) derivatives arose at t_R 17.2 min.⁵⁶ 1-O-Substituted fructose units (7.09%) were determined by the presence of 3,4,6- Me_3 -Glc (t_R 13.88 min) and 3,4,6- Me_3 -Man (t_R 13.95 min).⁵⁶

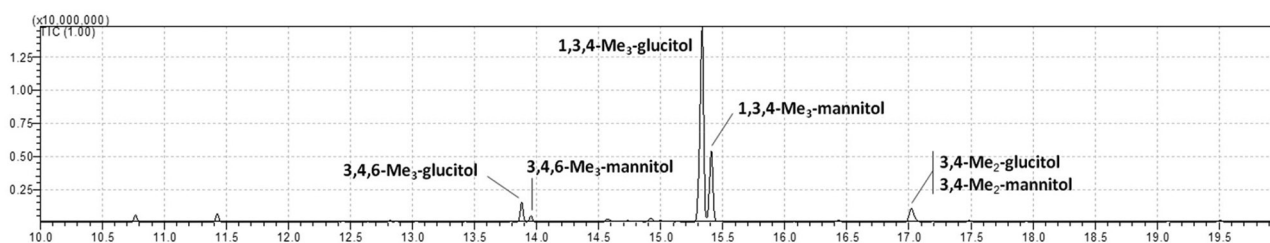


Figure 2. Chromatogram of the PMAA derivatives found for the levan produced by *Gluconobacter cerinus* UELBM11. 2,3,4,6- Me_4 -glucitol, 1,3,4,6- Me_4 -glucitol and 1,3,4,6- Me_4 -mannitol derivatives representing non-reducing terminals of *t*-GlcP and *t*-Fruf are not indicated in the chromatogram since they represent together < 1.5% of the total partially methylated alditol acetate (PMAA) derivatives found.

Table 2. Partially methylated alditol acetate (PMAA) derivatives found for the levan produced by *Gluconobacter cerinus* UELBM11

t_R / min	PMAA ^{a,b}	Main m/z signals	D-Fructose linkage on levan	Molar ratio / %
12.44	2,5-di- <i>O</i> -acetyl-1,3,4,6-tetra- <i>O</i> -methyl-glucitol	71, 87, 101, 129, 161	<i>t</i> -Fru f -(2→)	0.91
12.53	2,5-di- <i>O</i> -acetyl-1,3,4,6-tetra- <i>O</i> -methyl-mannitol			
13.88	1,2,5-tri- <i>O</i> -acetyl-3,4,6-tri- <i>O</i> -methyl-glucitol	87, 101, 117, 129, 145, 161	→1)-Fru f -(2→)	7.09
13.95	1,2,5-tri- <i>O</i> -acetyl-3,4,6-tri- <i>O</i> -methyl-mannitol			
15.32	2,5,6-tri- <i>O</i> -acetyl-1,3,4-tri- <i>O</i> -methyl-glucitol	87, 99, 101, 129, 161, 189	→6)-Fru f -(2→)	86.13
15.40	2,5,6-tri- <i>O</i> -acetyl-1,3,4-tri- <i>O</i> -methyl-mannitol			
17.20 ^c	1,2,5,6-tetra- <i>O</i> -acetyl-3,4-di- <i>O</i> -methyl-glucitol	87, 99, 129, 189	→1,6)-Fru f -(2→)	5.87
17.20 ^c	1,2,5,6-tetra- <i>O</i> -acetyl-3,4-di- <i>O</i> -methyl-mannitol			

^aPMAA derivatives obtained after permethylation with CH₃I, hydrolysis, reduction with NaBH₄ and acetylation. ^bThe derivative 1,5-di-*O*-acetyl-2,3,4,6-tetra-*O*-methyl-glucitol (< 0.5%) was also found at t_R = 12.39 min, representing the terminal glucopyranosyl non-reducing end of the levan. ^cBoth PMAA derivatives representing 1,6-di-*O*-substituted Fru f units on the levan structure were found co-eluted on the chromatogram.

Both terminal non-reducing units of the levan structure were found on the chromatogram as 2,3,4,6-Me₄-Glc_p at t_R 12.39 min (< 0.5%), indicating the D-glucopyranosyl terminal unit,³³ and as 1,3,4,6-Me₄-Glc and 1,3,4,6-Me₄-Man, found respectively at t_R 12.44 min and t_R 12.53 min, together accounting for 0.91% of the total of PMAA in the sample and representing the D-fructofuranosyl terminal units.⁵⁶

NMR spectroscopy

The sample of purified levan produced by *G. cerinus* UELBM11 was analyzed using ¹H NMR to obtain molecular structure details (Figure 3a).

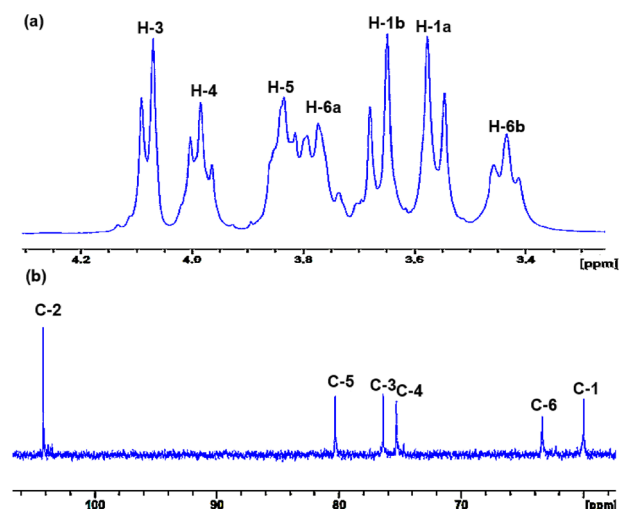


Figure 3. ¹H NMR (400 MHz, H₂O/D₂O at 5:1) (a) and ¹³C NMR (100 MHz, D₂O) (b) spectra of levan produced by *Gluconobacter cerinus* UELBM11.

The seven hydrogens found on fructofuranosyl backbone repeating units resonated between 3.7 and 4.1 ppm. Five out of them, were clearly observed at 3.45 (t, H-6b); 3.56 (d, H-1a); 3.67 (d, H-1b); 3.97 (t, H-4) and 4.07 ppm (d, H-3) while H-6a and H-5 signals appeared partially overlapped between 3.72 and 3.90 ppm. These

results corroborate the absorption bands previously found in the FTIR analysis.

The ¹³C NMR spectrum (Figure 3b) showed six signals, corresponding to each of the carbons found on D-fructofuranosyl repeating units (δ 104.2, 80.06, 76.40, 75.52, 63.75, and 60.25). The anomeric C-2 signal shown at δ 104.2 confirms the β configuration of D-Fru f /backbone units. The same chemical shift for the anomeric carbon was found by Joaquim *et al.*⁵⁷ where it has been demonstrated that levans are usually formed by repeating units of β -D-fructose linked glycosidic bonds at C-2 and C-6. The signals at δ 60.25 and 63.75 were assigned to the methylene groups C-1 and C-6, respectively. The chemical shift for C-5 in the furanoside ring arose at δ 80.06, and signals at δ 75.52 and 76.40 were attributed to the oxymethine groups (C-4 and C-3). These results confirm that levan from *G. cerinus* UELBM11 consists of a majorly linear β -D-fructofuranose polysaccharide with 2→6 glycosidic linkages forming the backbone structure. Signals of the minor β -D-fructose units branching the main structure at O-1 and terminal non-reducing units of D-glucopyranosyl found earlier during the GC-MS analyses were hardly observed in the NMR spectra due to their lower relative abundance in comparison to the β -(1→2)-D-Fru f /repeating units forming the main chain of the polysaccharide.

Thermal stability of levan by TGA/DTG profile

TGA analysis is a method that provides information related to the thermal stability of the samples from the change and/or rate of change in weight (DTG) as a function of temperature. The TGA and DTG results for the levan from *G. cerinus* UELBM11 are shown in Figure 4.

Thermal degradation of levans occurred in three stages. At the first stage, between 30 and 200 °C, approximately 12% of weight loss was observed, which may be attributed to residual moisture.¹² The second stage was directly associated with the thermal decomposition of fructans, which has been previously observed between 200 and 300 °C^{12,58,59} and

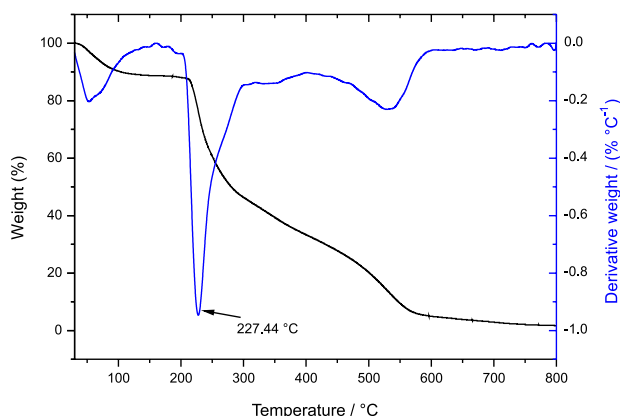


Figure 4. TGA and DTG as a function of temperature for levan from *Gluconobacter cerinus* UELBM11.

between 200 and 400 °C.⁶⁰ During this stage (200–300 °C), levan from *G. cerinus* UELBM11 showed a considerable weight loss (41.46%) and the highest rate of change of the derivative weight curve was observed precisely at 227.44 °C. Other authors have also reported the maximum decomposition rate over this temperature range, with derivative peak temperatures at 216.67⁵⁹ and 253 °C.⁵⁸ With the increment of the temperature from 300 to 400 °C, levan showed a lower weight loss of around 13.1%. According to Stivala *et al.*⁶¹ the decomposition at this stage is probably caused by the gradual breaking of levan β -(2→1) branching linkages and subsequent breakdown of the branching chains. After further heating, the more thermally resistant β -(2→6) backbone bonds and pyranose rings are broken. Finally, at the third stage (400–650 °C), ashes were detected, and approximately 30% of weight loss was observed, as similarly reported by Espinosa-Andrews and Rodríguez-Rodríguez.⁶⁰

The thermal characteristics of the levan from *G. cerinus* UELBM11 suggest that it could be a good additive for food applications since TGA/DTG displayed that the decomposition of fructans occurred at temperatures close to 200 °C and the numerous food preparations rarely

exceed 150 °C.⁶² Furthermore, levans could also be used as a stabilizing agent for pharmaceuticals/cosmeceutical formulations⁶³ and as a carrying agent for powdered foods.⁶⁴ Levan could act by protecting the active ingredients from thermal and environmental decomposition and, consequently, extending the shelf life of the product.⁶⁵

Morphology of levan determined using SEM

SEM has been a valuable tool for the examination of surface characteristics of polysaccharides and for the assistance in understanding their physical properties.⁶⁶ Figure 5 shows the microstructures of levan from *G. cerinus* UELBM11 (Figures 5a–5b), in which it is possible to observe a few rod-shaped structure and drop-like granules,⁶⁷ as well as a very pronounced microporous matrix.

This network appeared to be connected by several sheet layers, each with a significant number of nanopores with regular round or elliptical shapes. Previous studies reported a similar porous morphology in levans produced by *Brenneria* sp. EniD312,⁵⁹ *Erwinia amylovora*,⁶⁸ *Bacillus subtilis* natto KB1,⁵¹ and *Bacillus mojavensis*.⁶⁹ According to Haddar *et al.*⁶⁹ and Lobo *et al.*,⁶⁶ the microporosity allows greater water holding capacity, which makes levans an interesting component for cosmetics production.⁴³ Besides, these properties suggest that levan from *G. cerinus* UELBM11 can be a potential functional agent for enhancing thickening, gelling, stabilizing, emulsifying, and water-binding properties for the processing of foods.^{69,70}

Antioxidant capacity of levan

The ABTS•+ method is widely used to assess the radical scavenging capacities of hydrophilic and lipophilic antioxidants.⁶⁶ The ABTS•+ scavenging ability of levans produced by *G. cerinus* UELBM11 compared to that of vitamin C is shown in Figure 6a.

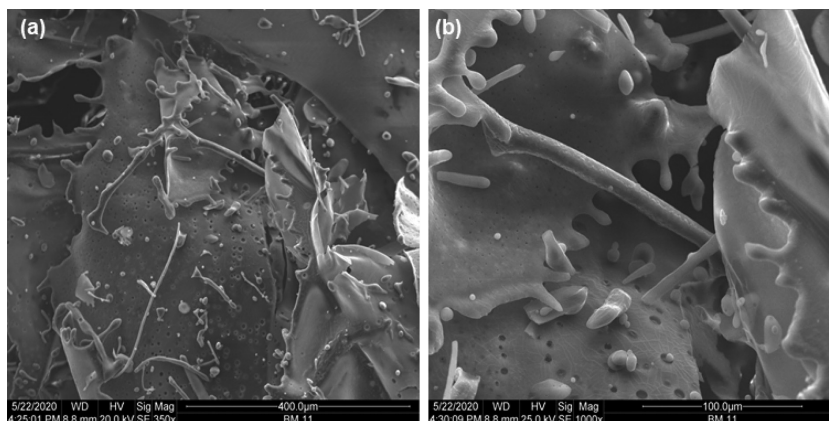


Figure 5. Scanning electron microscopy showing the surface microstructure formed by levan from *Gluconobacter cerinus* UELBM11 (a) 350 \times , (b) 1.000 \times .

Levan demonstrated potential as an antioxidant agent despite its lower inhibitory activity than vitamin C at all concentrations tested. It has been observed that the radical scavenging ability increased in a dose-dependent manner. *G. cerinus* levans reached nearly 50% of their scavenging activity at higher concentrations (0.9 mg mL⁻¹). This scavenging activity has been shown not to be as high as that of *Lactobacillus plantarum* KX041 (ca. 90%; 0.6 mg mL⁻¹),⁷¹ but it was similar to levan from *Bacillus megaterium* PFY-147 (ca. 50%; 1 mg mL⁻¹)⁵⁰ and higher than the activity found for the levan of *Bacillus licheniformis* (strain FRI MY-55) (ca. 15-20%; 2.5 mg mL⁻¹).³⁷ The ability of levan from *G. cerinus* UELBM11 to act as an antioxidant may be attributed to its large number of hydroxyl groups, which may convert reactive free radicals into more stable forms and halt the free radical chain reaction, most likely due to its ability to donate hydrogens.⁶²

Hydroxyl radicals are highly reactive compounds that destroy cellular components and macromolecules. This action results in accelerated aging and facilitates the occurrence and development of oxidative stress-related diseases.⁵⁰ Considering the importance of protecting the organism from free-radical damage, we also evaluated the *G. cerinus* UELBM11 levan ability to scavenge hydroxyl radicals. Figure 6b shows that the scavenging rates of both the levan sample and vitamin C were concentration-dependent. While vitamin C showed nearly 100% scavenging activity at 1.1 mg mL⁻¹, *G. cerinus* levans exhibited ca. 67% activity at the same concentration. The radical scavenging rate gradually stabilized as the levan concentration increased, reaching a maximum of 70.80% at 2.9 mg mL⁻¹. Similar to our findings, Liu *et al.*⁷² found a scavenging activity of 68.55% at the highest concentration of levan evaluated (1.0 mg mL⁻¹). Pei *et al.*⁵⁰ have also reported a scavenging effect close to the ones shown in this work (79.29%); however, only at much higher concentrations of levan (5.0 mg mL⁻¹). Furthermore, the results shown herein were shown to be more promising than those found for EPS produced by *Leuconostoc citreum* B-2 (12.92%

at 15 mg mL⁻¹)⁷³ and the levan from *Bacillus licheniformis* (strain FRI MY-55) (15% at 2.5 mg mL⁻¹).³⁷ It is possible that the levan from *G. cerinus* UELBM11 has reduced the ferrous ion concentration that promotes the Fenton's reaction and that its scavenging effects have been due to its ability to donate active hydrogen through hydroxyl substitutions.⁶² These findings showed that levan from *G. cerinus* UELBM11 has a significant effect on radical scavenging and is a potential candidate for use as a natural alternative to commercial antioxidants.

Conclusions

We identified five isolates belonging to the genus *Gluconobacter*. *G. cerinus* UELBM11 exhibited the highest levan production yield (13.89 g L⁻¹) under non-optimized conditions. The structure of levan from *G. cerinus* UELBM11 is mainly composed of β-(2→6)-D-fructofuranosyl repeating units with very few β-D-Fruf branching units found at O-1 and had a molecular weight of 8.78 × 10⁵ Da. In addition, this levan was revealed to form a microporous structure, show excellent thermal properties and stability, and have enormous potential as a free radical scavenger, particularly owing to its high hydroxyl radical scavenging ability. Hence, the authors have shown herein the versatility of AAB and the potential of *G. cerinus* UELBM11 to produce polysaccharides such as levan, which, in addition to its bioactive natural antioxidant properties, may also be used as an additive in cosmetics, pharmaceuticals, and food products.

Supplementary Information

Supplementary data are available free of charge at <http://jbcs.sbq.org.br> as PDF file.

Acknowledgments

The authors thank the Laboratory of Electronic

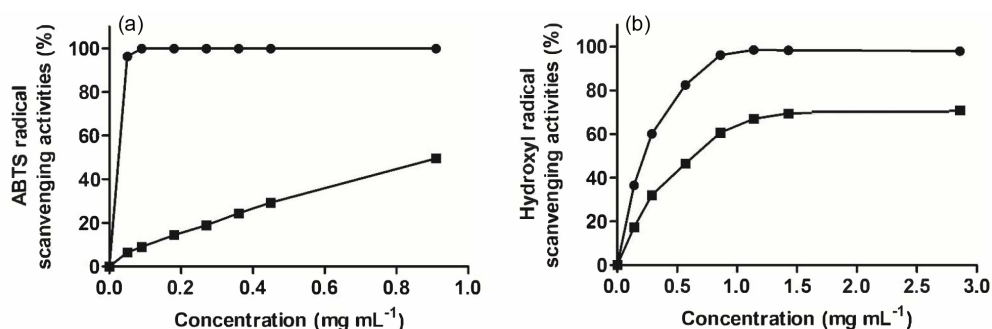


Figure 6. Antioxidant activities by scavenging activity of the radicals: ABTS (a) and hydroxyl (b) from levan by *Gluconobacter cerinus* UELBM11 (■) and vitamin C (●). Data are presented as the mean ± standard deviation of independent triplicates.

Microscopy and Microanalysis (LMEM-UEL) for performing the scanning microscopy analyses. We thank the National Council of Technological and Scientific Development (CNPq) for providing a scholarship to Natália N. Y. Hata (grant number: 142379/2017-4). FAM thanks the CNPq/National Institute of Science and Technology (INCT) (process 465357/2014-8).

Author Contributions

Natália N. Y. Hata was responsible for conceptualization, data curation, formal analysis, investigation, methodology, project administration, validation, visualization, writing (original draft, review and editing); Daniele Sartori for formal analysis, funding acquisition, investigation, methodology, resources, validation, visualization, and writing (review and editing); Matheus Mertz Ribeiro for methodology; Rodrigo V. Serrato for investigation, methodology, validation, visualization, writing (original draft, review and editing); Adriana A. B. Tomal for investigation, methodology, validation, visualization, writing (original draft, and review and editing); Leonel Vinícius Constantino for investigation, methodology, validation, visualization, and writing-review; Mariana Assis de Queiroz Cancian for investigation, and methodology; Francisco de Assis Marques for resources, writing-review and editing; Fernando Teruhiko Hata for investigation, writing-review and editing; Fernanda Carla Henrique Bana for methodology, and investigation; Fernando César de Macedo Júnior for investigation, and methodology; Wilma A. Spinosa for conceptualization, data curation, formal analysis, funding acquisition, investigation, resources, supervision, validation, visualization, and writing-review and editing.

References

- De Roos, J.; De Vuyst, L.; *Curr. Opin. Biotechnol.* **2018**, *49*, 115. [Crossref]
- Valera, M. J.; Laich, F.; González, S. S.; Torija, M. J.; Mateo, E.; Mas, A.; *Int. J. Food Microbiol.* **2011**, *151*, 105. [Crossref]
- Lynch, K. M.; Zannini, E.; Wilkinson, S.; Daenen, L.; Arendt, E. K.; *Compr. Rev. Food Sci. Food Saf.* **2019**, *18*, 587. [Crossref]
- Aramsangtienchai, P.; Kongmon, T.; Pechroj, S.; Srisook, K.; *Int. J. Biol. Macromol.* **2020**, *163*, 574. [Crossref]
- Mantovan, J.; Bersaneti, G. T.; Faria-Tischer, P. C. S.; Celligoi, M. A. P. C.; Mali, S.; *Food Packag. Shelf Life* **2018**, *18*, 31. [Crossref]
- Ni, D.; Xu, W.; Bai, Y.; Zhang, W.; Zhang, T.; Mu, W.; *Int. J. Biol. Macromol.* **2018**, *113*, 29. [Crossref]
- Bersaneti, G. T.; Pan, N. C.; Baldo, C.; Celligoi, M. A. P. C.; *Appl. Biochem. Biotechnol.* **2018**, *184*, 838. [Crossref]
- Küçüktaşık, F.; Kazak, H.; Güney, D.; Finore, I.; Poli, A.; Yenigün, O.; Nicolaus, B.; Öner, E. T.; *Appl. Microbiol. Biotechnol.* **2011**, *89*, 1729. [Crossref]
- Liu, C.; Kolida, S.; Charalampopoulos, D.; Rastall, R. A.; *J. Funct. Foods* **2020**, *64*, 103668. [Crossref]
- Jakob, F.; Steger, S.; Vogel, R. F.; *Eur. Food Res. Technol.* **2012**, *234*, 493. [Crossref]
- Öner, E. T.; Hernández, L.; Combie, J.; *Biotechnol. Adv.* **2016**, *34*, 827. [Crossref]
- Srikanth, R.; Siddartha, G.; Reddy, C. H. S. S.; Harish, B. S.; Ramaiah, M. J.; Uppuluri, K. B.; *Carbohydr. Polym.* **2015**, *123*, 8. [Crossref]
- Sarilmiser, H. K.; Öner, E. T.; *Biochem. Eng. J.* **2014**, *92*, 28. [Crossref]
- Gamal, A. A.; Abbas, H. Y.; Abdelwahed, N. A. M.; Kashef, M. T.; Mahmoud, K.; Esawy, M. A.; Ramadan, M. A.; *Int. J. Biol. Macromol.* **2021**, *182*, 1590. [Crossref]
- Ragab, T. I. M.; Shalaby, A. S. G.; Awdan, S. A. E.; El-Bassouni, G. T.; Salama, B. M.; Helmy, W. A.; Esawy, M. A.; *Int. J. Biol. Macromol.* **2020**, *142*, 564. [Crossref]
- Sokollek, S. J.; Hertel, C.; Hammes, W. P.; *J. Biotechnol.* **1998**, *60*, 195. [Crossref]
- Yamada, Y.; Hosono, R.; Lisdyanti, P.; Widyastuti, Y.; Saono, S.; Uchimura, T.; Komagata, K.; *J. Gen. Appl. Microbiol.* **1999**, *45*, 23. [Crossref]
- Sievers, M.; Swings, J.; *Acetobacteraceae In Bergey's Manual of Systematics of Archaea and Bacteria*; John Wiley & Sons: Chichester, UK, 2015. [Crossref]
- Sievers, M.; Swings, J.; *Gluconobacter In Bergey's Manual of Systematics of Archaea and Bacteria*; John Wiley & Sons: Chichester, UK, 2015. [Crossref]
- Asai, T.; Iizuka, H.; Komagata, K.; Asap, T.; Komagata, K.; *J. Gen. Appl. Microbiol.* **1964**, *10*, 95. [Crossref]
- Cirigliano, M. C.; *J. Food Sci.* **1982**, *47*, 1038. [Crossref]
- Fugelsang, K.; Edwards, C.; *Wine Microbiology, Practical Applications and Procedures*, 2nd ed.; Springer, 2007, p. 241. [Crossref]
- Cheng, H. R.; Jiang, N.; *Biotechnol. Lett.* **2006**, *28*, 55. [Crossref]
- Ruiz, A.; Poblet, M.; Mas, A.; Guillamón, J. M.; *Int. J. Syst. Evol. Microbiol.* **2000**, *50*, 1981. [Crossref]
- National Center for Biotechnology Information PubChem, <https://pubchem.ncbi.nlm.nih.gov/>, accessed in August 2024.
- Kumar, S.; Stecher, G.; Tamura, K.; *Mol. Biol. Evol.* **2016**, *33*, 1870. [Crossref]
- Hestrin, S.; Schramm, M.; *Biochem. J.* **1954**, *58*, 345. [Crossref]
- Serrato, R. V.; Meneses, C. H. S. G.; Vidal, M. S.; Santana-Filho, A. P.; Iacomini, M.; Sasaki, G. L.; Baldani, J. I.; *Carbohydr. Polym.* **2013**, *98*, 1153. [Crossref]
- DuBois, M.; Gilles, K. A.; Hamilton, J. K.; Rebers, P. A.; Smith, F.; *Anal. Chem.* **1956**, *28*, 350. [Crossref]
- Bradford, M. M.; *Anal. Chem.* **1976**, *72*, 248. [Crossref]

31. Semjonovs, P.; Shakirova, L.; Treimane, R.; Shvirksts, K.; Auzina, L.; Cleenwerck, I.; Zikmanis, P.; *Lett. Appl. Microbiol.* **2016**, *62*, 145. [Crossref]
32. *ASTRA*, version 4.70.07; Wyatt Technology, Waters Corporation, Santa Barbara, CA, 1998.
33. Dong, C. X.; Zhang, L. J.; Xu, R.; Zhang, G.; Zhou, Y. B.; Han, X. Q.; Zhang, Y.; Sun, Y. X.; *Int. J. Biol. Macromol.* **2015**, *77*, 99. [Crossref]
34. Gojgic-Cvijovic, G. D.; Jakovljevic, D. M.; Loncarevic, B. D.; Todorovic, N. M.; Pergal, M. V.; Ciric, J.; Loos, K.; Beskoski, V. P.; Vrvic, M. M.; *Int. J. Biol. Macromol.* **2019**, *121*, 142. [Crossref]
35. Bouallegue, A.; Casillo, A.; Chaari, F.; La Gatta, A.; Lanzetta, R.; Corsaro, M. M.; Bachoual, R.; Ellouz-Chaabouni, S.; *Int. J. Biol. Macromol.* **2020**, *144*, 316. [Crossref]
36. Sasaki, G. L.; Gorin, P. A. J.; Souza, L. M.; Czelusniak, P. A.; Iacomini, M.; *Carbohydr. Res.* **2005**, *340*, 731. [Crossref]
37. Huang, T. Y.; Huang, M. Y.; Tsai, C. K.; Su, W. T.; *J. Biosci. Bioeng.* **2020**, *131*, 98. [Crossref]
38. Gomaa, M.; Yousef, N.; *Int. J. Biol. Macromol.* **2020**, *149*, 552. [Crossref]
39. *Statistica*, version 10; StatSoft, Tulsa, USA, 2011.
40. *GraphPad Prism*, version 5.0; GraphPad Software Inc., San Diego, USA, 2007.
41. *Origin*, version 8.0; OriginLab Corporation, Origin Pro, Northampton, USA, 2019.
42. Ua-Arak, T.; Jakob, F.; Vogel, R. F.; *Front. Microbiol.* **2017**, *8*, 807. [Crossref]
43. Moussa, T. A. A.; Al-Qaysi, S. A. S.; Thabit, Z. A.; Kadhem, S. B.; *Process Biochem.* **2017**, *57*, 9. [Crossref]
44. Jakob, F.; Pfaff, A.; Novoa-Carballal, R.; Rüksam, H.; Becker, T.; Vogel, R. F.; *Carbohydr. Polym.* **2013**, *92*, 1234. [Crossref]
45. Lakra, A. K.; Domdi, L.; Tilwani, Y. M.; Arul, V.; *Int. J. Biol. Macromol.* **2020**, *143*, 797. [Crossref]
46. Ortiz-Soto, M. E.; Porras-Domínguez, J. R.; Seibel, J.; López-Munguía, A. L. M.; *Carbohydr. Polym.* **2019**, *219*, 130. [Crossref]
47. Zhang, X.; Liang, Y.; Yang, H.; Yang, H.; Chen, S.; Huang, F.; Hou, Y.; Huang, R.; *LWT* **2021**, *150*, 111951. [Crossref]
48. Yamamoto, Y.; Takahashi, Y.; Kawano, M.; Iizuka, M.; Matsumoto, T.; Saeki, S.; Yamaguchi, H.; *J. Nutr. Biochem.* **1999**, *10*, 13. [Crossref]
49. Salama, B. M.; Helmy, W. A.; Ragab, T. I. M.; Ali, M. M.; Taie, H. A. A.; Esawy, M. A.; *J. Basic Microbiol.* **2019**, *59*, 1004. [Crossref]
50. Pei, F.; Ma, Y.; Chen, X.; Liu, H.; *Int. J. Biol. Macromol.* **2020**, *161*, 1181. [Crossref]
51. Domżał-Kędzia, M.; Lewińska, A.; Jaromin, A.; Weselski, M.; Pluskota, R.; Łukaszewicz, M.; *Bioorg. Chem.* **2019**, *93*, 102787. [Crossref]
52. Tilwani, Y. M.; Lakra, A. K.; Domdi, L.; Yadav, S.; Jha, N.; Arul, V.; *Process Biochem.* **2021**, *110*, 282. [Crossref]
53. Han, J.; Feng, H.; Wang, X.; Liu, Z.; Wu, Z.; *BMC Biotechnol.* **2021**, *21*, 14. [Crossref]
54. Čopíková, J.; Barros, A. S.; Šmídová, I.; Černá, M.; Teixeira, D.; Delgadillo, I.; Synytsya, A.; Coimbra, M. A.; *Carbohydr. Polym.* **2006**, *63*, 355. [Crossref]
55. Liu, C.; Lu, J.; Lu, L.; Liu, Y.; Wang, F.; Xiao, M.; *Bioresour. Technol.* **2010**, *101*, 5528. [Crossref]
56. Cai, G.; Liu, Y.; Li, X.; Lu, J.; *J. Agric. Food Chem.* **2019**, *67*, 8029. [Crossref]
57. Joaquim, E. O.; Hayashi, A. H.; Torres, L. M. B.; Figueiredo-Ribeiro, R. C. L.; Shiomi, N.; Sousa, F. S.; Lago, J. H. G.; Carvalho, M. A. M.; *Front. Plant Sci.* **2018**, *9*, 1745. [Crossref]
58. Poli, A.; Kazak, H.; Gürleyendağ, B.; Tommonaro, G.; Pieretti, G.; Öner, E. T.; Nicolaus, B.; *Carbohydr. Polym.* **2009**, *78*, 651. [Crossref]
59. Xu, W.; Liu, Q.; Bai, Y.; Yu, S.; Zhang, T.; Jiang, B.; Mu, W.; *Int. J. Biol. Macromol.* **2018**, *109*, 810. [Crossref]
60. Espinosa-Andrews, H.; Rodríguez-Rodríguez, R.; *J. Therm. Anal. Calorim.* **2018**, *132*, 197. [Crossref]
61. Stivala, S. S.; Kimura, J.; Reich, L.; *Thermochim. Acta* **1981**, *50*, 111. [Crossref]
62. Farinazzo, F. S.; Valente, L. J.; Almeida, M. B.; Simionato, A. S.; Fernandes, M. T. C.; Mauro, C. S. I.; Tomal, A. A. B.; Garcia, S.; *Process Biochem.* **2020**, *91*, 141. [Crossref]
63. Sreenivasan, S.; Kandasamy, R.; *Int. J. Pept. Res. Ther.* **2017**, *23*, 305. [Crossref]
64. Booten, K.; De Soete, J.; Booten, A. F.; *Eur. pat. 0821885A1*, **1998**.
65. Leyva-Porras, C.; Cruz-Alcantar, P.; Espinosa-Sol, V.; Saavedra-Leos, M. Z.; *Polymers* **2019**, *12*, 5. [Crossref]
66. Lobo, R. E.; Gómez, M. I.; Valdez, G. F.; Torino, M. I.; *Food Hydrocolloids* **2019**, *96*, 625. [Crossref]
67. Kekez, B.; Gojgic-Cvijovic, G.; Jakovljevic, D.; Pavlović, V.; Beškoski, V.; Popović, A.; Vrvic, M. M.; Nikolić, V.; *Carbohydr. Polym.* **2016**, *154*, 20. [Crossref]
68. Xu, W.; Peng, J.; Ni, D.; Zhang, W.; Wu, H.; Mu, W.; *Carbohydr. Polym.* **2020**, *234*, 115921. [Crossref]
69. Haddar, A.; Hamed, M.; Bouallegue, A.; Bastos, R.; Coelho, E.; Coimbra, M. A.; *Food Chem.* **2020**, *343*, 128456. [Crossref]
70. Feng, F.; Zhou, Q.; Yang, Y.; Zhao, F.; Du, R.; Han, Y.; Xiao, H.; Zhou, Z.; *Int. J. Biol. Macromol.* **2018**, *113*, 45. [Crossref]
71. Wang, X.; Shao, C.; Liu, L.; Guo, X.; Xu, Y.; Lü, X.; *Int. J. Biol. Macromol.* **2017**, *103*, 1173. [Crossref]
72. Liu, J.; Luo, J.; Ye, H.; Zeng, X.; *Food Chem. Toxicol.* **2012**, *50*, 767. [Crossref]
73. Wang, Y.; Du, R.; Qiao, X.; Zhao, B.; Zhou, Z.; Han, Y.; *Int. J. Biol. Macromol.* **2020**, *142*, 73. [Crossref]

Submitted: May 9, 2024

Published online: August 30, 2024